



HAL
open science

Impact of air quality model settings for the evaluation of emission reduction strategies to curb air pollution

Bertrand Bessagnet, Elissavet Bossioli, Arineh Cholakian, Marta García Vivanco, Kees Cuvelier, Mark Theobald, Victoria Gil, Laurent Menut, Alexander de Meij, Enrico Pisoni, et al.

► To cite this version:

Bertrand Bessagnet, Elissavet Bossioli, Arineh Cholakian, Marta García Vivanco, Kees Cuvelier, et al.. Impact of air quality model settings for the evaluation of emission reduction strategies to curb air pollution. *Environmental Research*, 2024, 255, pp.119112. 10.1016/j.envres.2024.119112 . hal-04727827

HAL Id: hal-04727827

<https://cnrs.hal.science/hal-04727827v1>

Submitted on 10 Oct 2024

HAL is a multi-disciplinary open access archive for the deposit and dissemination of scientific research documents, whether they are published or not. The documents may come from teaching and research institutions in France or abroad, or from public or private research centers.

L'archive ouverte pluridisciplinaire **HAL**, est destinée au dépôt et à la diffusion de documents scientifiques de niveau recherche, publiés ou non, émanant des établissements d'enseignement et de recherche français ou étrangers, des laboratoires publics ou privés.



Distributed under a Creative Commons Attribution 4.0 International License



Impact of air quality model settings for the evaluation of emission reduction strategies to curb air pollution

Bertrand Bessagnet^{a,*}, Elissavet Bossioli^b, Arineh Cholakian^c, Marta García Vivanco^d, Kees Cuvelier^{a,1}, Mark R. Theobald^d, Victoria Gil^d, Laurent Menut^c, Alexander de Meij^e, Enrico Pisoni^a, Philippe Thunis^a

^a European Commission, Joint Research Centre, Via Enrico Fermi, Ispra, 21017, Varese, Italy

^b Department of Physics, Sector of Environmental Physics & Meteorology, National and Kapodistrian University of Athens, Athens, Greece

^c Laboratoire de Météorologie Dynamique (LMD), Ecole Polytechnique, IPSL Research University, Ecole Normale Supérieure, Université Paris-Saclay, Sorbonne Universités, UPMC Univ Paris 06, CNRS, Route de Saclay, Palaiseau, 91128, France

^d Atmospheric Modelling Unit, Environment Department, CIEMAT, Avda. Complutense, 40, Madrid, 28040, Spain

^e METCLIM, Varese, Italy

ARTICLE INFO

Keywords:

Modeling
Emission reduction
Chemistry
Resolution
Air quality
Meteorology

ABSTRACT

For air quality management, while numerical tools are mainly evaluated to assess their performances on absolute concentrations, this study assesses the impact of their settings on the robustness of model responses to emission reduction strategies for the main criteria pollutants. The effect of the spatial resolution and chemistry schemes is investigated. We show that whereas the spatial resolution is not a crucial setting (except for NO₂), the chemistry scheme has more impact, particularly when assessing hourly values of the absolute potential of concentrations. The analysis of model responses under the various configurations triggered an analysis of the impact of using online models, like WRF-chem or WRF-CHIMERE, which accounts for the impact of aerosol concentrations on meteorology. This study informs the air quality modeling community on what extent some model settings can affect the expected model responses to emission changes. We suggest to not activate online effects when analyzing the effect of an emission reduction strategy to avoid any confusion in the interpretation of results even if an online simulation should represent better the reality.

1. Introduction

Air pollution is a silent threat for human and ecosystem health. The World Health Organization (WHO) estimated, for 2019 (WHO, 2023), that 6.7 million premature deaths were attributed to ambient and household air pollution from particulate matter (PM) with a diameter less than 2.5 μm (PM_{2.5}). In 2021, the WHO updated the air quality guidelines (WHO, 2021) with more stringent thresholds (AQG), reflecting updated evidence that air pollution is associated with adverse health effects at lower concentrations than previously recognized. The recommended annual mean PM_{2.5} level was reduced from 10 to 5 μg m⁻³, and from 20 to 15 μg m⁻³ for PM₁₀. Despite undeniable improvements in air quality, levels of air pollutant concentrations above EU standards still occur in Europe and air pollution remains a major health concern for Europeans (EEA, 2023). Furthermore, the new WHO guidelines will foster the development of new actions to improve air quality.

Modeling tools like chemistry transport models (CTM) are commonly used to assess emission reduction strategies. These models are evaluated against observations (Eder et al., 2010; Eder and Yu, 2006; Curci, 2012; Bessagnet et al., 2023) and many studies tackle the impact of chemical and physical processes, initial and boundary conditions, or emissions on absolute concentrations or trends but rarely in terms of responses to an emission reduction. The FAIRMODE (Kushtha et al., 2019) forum supports the Air Quality directive to guide model users in this regulation context. A recent work (Bessagnet et al., 2023) presented a platform to evaluate the model responses to emission changes down to the urban scale. Another complementary study (De Meij et al., 2024) assessed the sensitivity of model responses to the emission input. This study revealed that reducing gas and aerosol precursors of O₃ and PM₁₀ concentrations, respectively, led to different potentials and potencies. This can mainly be explained by the differences in emission quantities, differences in their spatial distributions as well as in their sector allocation. These studies have revealed a large variability in

* Corresponding author.

E-mail address: bertrand.bessagnet@lmd.ipsl.fr (B. Bessagnet).

¹ Retired with Active Senior Agreement.

<https://doi.org/10.1016/j.envres.2024.119112>

Received 9 February 2024; Received in revised form 9 April 2024; Accepted 7 May 2024

Available online 22 May 2024

0013-9351/© 2024 The Author(s). Published by Elsevier Inc. This is an open access article under the CC BY license (<http://creativecommons.org/licenses/by/4.0/>).

responses even when the reduction was applied to inert precursors like primary PM.

In this follow-up study of Bessagnet et al. (2023), we have selected three urban areas (Paris, Madrid and Athens) to assess the impact of specific model settings on model responses to emission changes: particularly the horizontal resolution and the chemistry schemes. Horizontal resolution has been identified as a parameter to improve the performances of models. For non-linear components of the equations representing the physical and chemical processes, the spatial resolution is supposed to have an impact. However, in Bessagnet et al. (2023) and Colette et al. (2014) it has been identified that improving only the resolution does not improve necessarily the performances. Also, chemical schemes are very different and can be constructed in very different way. In this study, the sensitivity on chemical scheme is studied over Athens with RADM2 (Regional Acid Deposition Model, version 2) (Stockwell et al., 1990) and the RACM (Regional Atmospheric Chemistry Mechanism) (Stockwell et al., 1997). RADM2 yielded the lowest O₃ levels; the differences in O₃ precursors among the various mechanisms were insignificant under clean conditions and more profound under polluted conditions (Gross and Stockwell, 2003). Chen et al. (2021) shows large differences between Ozone peaks simulated by RACM and RADM2 mechanisms in a recent study over Taiwan. SAPRC (Statewide Air Pollution Research Center) version 7 (Carter, 2010) and MELCHIOR schemes on board CHIMERE (Menut et al., 2021) are used over the summer Madrid. MELCHIOR is the historical chemical scheme of CHIMERE while SAPRC has been introduced more recently.

In Bessagnet et al. (2023), we have identified some key model settings to better understand the variability which was observed. In this study, we analyze the change of a single model setting makes it easier to explain the overall variability in model responses. Two models, WRF-CHIMERE and WRF-chem, were selected and tested under various configurations and versions over the three urbanized areas in Europe previously mentioned.

2. Method

2.1. Methodology

The models have already been validated in Bessagnet et al. (2023), where the full description of the exercise is presented. The selection of episodes is explained in Bessagnet et al. (2023). More specifically, both winter and summer episodes were selected to highlight the seasonal dependency of emissions and their interaction with the different meteorological conditions prevailing during each period. Each episode covers a few days and is selected on the basis of the CAMS reports and other observational data. Even though the aim of this publication was not to validate the models, a comprehensive supplementary file A was provided that gives information on model performances. To summarize the performances of models, we show that correlations for Ozone on hourly basis is close to 0.75 for CHIMERE for Paris and Madrid base cases but lower over Athens (usually below 0.50). Winter episodes show the best performances for PM compared to summer cases with particularly good correlations and root mean square errors for CHIMERE over Paris. A large bias is observed for NO₂ concentrations simulated by WRFNKUA. In general, increasing the resolution does not improve automatically the performances, except for NO₂.

The general principle of the exercise is, for pollutant episodes of the year 2015, to analyze the model responses to a reduction of precursor emissions over the three urban areas displayed in Fig. 1. These three areas have been selected because they represent the diversity of geographical/climatological conditions in Europe, (i) a densely populated area over a rather flat zone (Paris), (ii) a large capital city at medium altitude (Madrid), and (iii) a major coastal city (Athens). Only three constraints are imposed on the modeling teams: (i) the dates of the air pollution episodes in 2015, (ii) the target domains over which emissions are reduced (Table 1) and, (iii) the precursor emissions that are reduced

and the strength of the reductions (−25 or −50%). All other model settings and forcing are up to the modeling teams.

For the various model configurations and list of episodes defined in Table 2, we analyze the model responses in terms of concentration deltas for a scenario where precursor emissions are reduced by $\alpha = 25\%$ or 50% for all activity sectors. These theoretical scenarios represent emission reductions that have a substantial impact on concentrations. For wintertime PM episodes, PPM (Primary Particulate Matter), NO_x (nitrogen oxides), SO_x (sulfur oxides), NH₃ (Ammonia) and VOC (Volatile Organic Compounds) precursor emissions were reduced, while for summer O₃ episodes, only reductions of NO_x and VOC precursors are considered. Emission reductions are applied from 00:00 UTC on the first day to 23:00 UTC on the last day of each episode. An additional scenario is performed in which all precursors are reduced simultaneously (denoted as ALL), i.e. PPM (Primary Particulate Matter), NO_x, SO_x, NH₃, VOC during winter (W) episodes, and NO_x and VOC during summer (S) episodes. The latter is useful to analyze the “additivity” (defined in Appendix A) of the effect of emission reductions. In this study, we will focus on the 50% emission reduction with straightforward names referring to scenarios as: 50%NOX, 50%NH3, 50%SOX, 50%PPM, 50%VOC and 50%ALL. The 25% emission reductions are used to analyze the “linearity” of the effect of emission reductions highlighting the non-linear processes.

Several indicators have been defined for analyzing modeled concentration changes in response to emission changes, namely the potential and potency (Thunis and Clappier, 2014; Thunis et al., 2015). These indicators are the most suitable for an analysis of model responses to emission changes thanks to a scaling with the emission reduction intensity and quantity of reduced emissions, respectively. The absolute potential (APL) is defined as the difference of a model variable V between a scenario and a base case normalized by the percentage α of the emission reduction $APL = \Delta V/\alpha$. We extend here the concept of “potential” initially dedicated to concentrations $V = C$, e.g. to meteorological variables or any others. The relative potential (RPL) is a normalization of the APL by the variable value V_{bc} of the base case: $RPL = \Delta V/(\alpha V_{bc})$. The absolute potency APY for concentrations is defined as $APY = \Delta C/(\alpha E)$, e.g. the delta of concentrations divided by the quantity of reduced emissions. These indicators can be applied to mean, median or percentile concentrations for the analyses. They can be either negative or positive showing a decrease or an increase of concentrations, respectively. In our analysis, we will also evaluate the impact of model settings by calculating the difference between the results obtained with two configurations, (1) and (2) as $\Delta APL = APL_2 - APL_1$. Note that APL_1 and APL_2 are associated with different base cases as the choice of configuration also affects the base case. Two ratios, *Linearity* and *additivity*, are defined in Appendix A to complement the analysis.

To explain the model behaviors on inorganic species, the *Gratio* (Ansari, 1999; Bessagnet et al., 2014) variable is used to distinguish chemical regimes based on secondary inorganic aerosol formation. It is defined as the ratio between free ammonia and total nitrate expressed in molar basis as in Eq. (1).

$$Gratio = \frac{(\text{NH}_4 + \text{NH}_3) - 2 \times \text{SO}_4}{(\text{NO}_3 + \text{HNO}_3)} \quad (1)$$

- *Gratio* > 1 indicates that nitric acid is limiting,
- *Gratio* < 0 indicates the ammonia is severely limiting,
- *Gratio* between 0 and 1 indicates ammonia is available for reaction with nitric acid, but ammonia is the limiting species.

For the summer episodes we have computed the VOC/NO_x ratio for some model configurations, also on a molar basis since it characterizes the chemical regime for ozone formation, VOC being expressed as concentration of carbon (C).

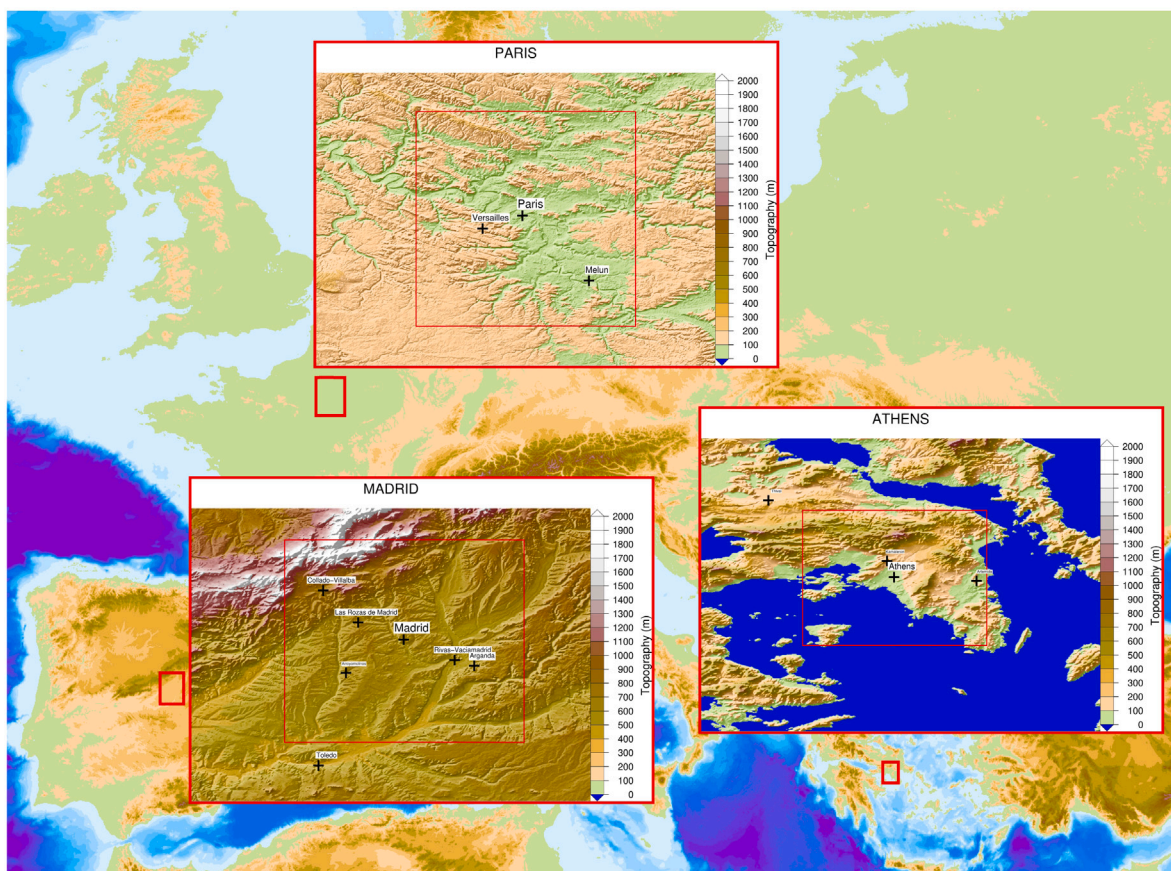


Fig. 1. Selected domains.

Table 1

List of selected domains defined by 4 corners in longitude and latitude where the emissions are reduced.

Country	City	Lon. Min. (°E)	Lon. Max. (°E)	Lat. Min. (°N)	Lat. Max. (°N)	City area (km ²)
France	Paris	+1.80	+2.90	+48.30	+49.40	12 098
Greece	Athens	+23.43	+24.03	+37.68	+38.28	3030
Spain	Madrid	-4.15	-3.25	+39.96	+40.86	6825

Table 2

Episode codes with corresponding city and time frame in 2015.

Codes	City	City abr.	Period	Episode season ^a
ATH016	Athens	ATH	6-14/08	S
PAR014	Paris	PAR	10-16/02	W
PAR015	Paris	PAR	5-6/06	S
MAD021	Madrid	MAD	22-23/01	W
MAD043	Madrid	MAD	1-5/07	S

^a Summer (S) or Winter (W) episodes.

2.2. Model configurations

The three main model configurations are detailed below. The configuration name used for each modeling team WRFNKUA, CHIMLMD and CHIMCIE is extended with a suffix related to resolution and/or chemistry as detailed in Table 3. The configuration acronym is composed of (i) the model name CHIM and WRF respectively for CHIMERE and WRFchem, (ii) followed by the name of the modeling group running the model CIE (for CIEMAT), LMD and NKUA, (iii) followed by the resolution in 100th degree or km and (iv) with a last suffix (if any) as a letter referring to the chemical scheme when the simulations are used to analyze the impact of the chemical scheme. A summary of model settings is provided in Table 4. In supplementary material D

are highlighted the differences on total emissions for each domain, pollutant, period and model configuration. Some small differences are displayed when the resolution changes for a given domain due to some interpolation issues. For CHIMERE, some differences are noticeable over Paris for SO_x and NH₃ emissions comparing the configurations from CIEMAT and LMD with 3 times lower emissions of ammonia emissions for the LMD emissions while SO_x emissions are higher for this configuration. Also, over Athens NO_x emissions are much higher (and lower for VOC) compared to the CHIMERE configurations which can explain the large bias observed previously when we have compared with the available observations.

WRF-Chem operated by NKUA — WRFNKUA

The model configuration is based on the Weather Research and Forecasting (WRF) model, Version 4.2, fully coupled with chemistry and aerosols, a modeling system that is extensively used in research studies. WRF-Chem simulations account for both the direct and indirect effect of aerosols (Grell et al., 2005). Four domains with horizontal resolutions of about 55.5 km, 18.5 km, 6 km and 2 km over Athens, respectively, are used, where the three inner domains are all two-way nested to their parent domain. Athens is the innermost domain. The latitude/longitude projection is used. In the vertical, 40 terrain-following sigma levels, with the lowest model level at about 14 m. The RRTMG scheme for the Longwave & Shortwave radiation (Iacono et al., 2008) and the Yonsei University Planetary Boundary layer

Table 3
Summary of model configurations.

Configuration	Resolution-Nesting ^a	Chemistry ^c	Cities-Period ^d
CHIMCIE01M	0.01° - 4 nesting	MELCHIOR	PAR-S/W, MAD-S/W, ATH-S
CHIMCIE01S	0.01° - 4 nesting	SAPRC	PAR-S/W, MAD-S/W, ATH-S
CHIMCIE03M	0.03° - 3 nesting	MELCHIOR	PAR-S/W, MAD-S/W, ATH-S
CHIMCIE03S	0.03° - 3 nesting	SAPRC	PAR-S/W, MAD-S/W, ATH-S
CHIMCIE09M	0.09° - 2 nesting	MELCHIOR	PAR-S/W, MAD-S/W, ATH-S
CHIMCIE09S	0.09° - 2 nesting	SAPRC	PAR-S/W, MAD-S/W, ATH-S
CHIMCIE27M	0.27° - 1 nesting	MELCHIOR	PAR-S/W, MAD-S/W, ATH-S
CHIMCIE27S	0.27° - 1 nesting	SAPRC	PAR-S/W, MAD-S/W, ATH-S
CHIMLMD03 ^b	3 km - 3 nesting	MELCHIOR	PAR-W
CHIMLMD10	10 km - 2 nesting	MELCHIOR	PAR-W
CHIMLMD30	30 km - 1 nesting	MELCHIOR	PAR-W
WRFNKUA02A	2 km - 4 nesting	RADM2-n	ATH-S
WRFNKUA02D	0.019° - 4 nesting	RADM2-o	ATH-S
WRFNKUA06A ^e	0.056° - 3 nesting	RADM2-n	ATH-S
WRFNKUA06B ^e	0.056° - 2 nesting	RACM-n	ATH-S
WRFNKUA06C ^e	0.056° - 2 nesting	RADM2-n	ATH-S
WRFNKUA06D ^e	0.056° - 3 nesting	RADM2-o	ATH-S
WRFNKUA18A	0.17° - 2 nesting	RADM2-n	ATH-S
WRFNKUA18B	0.17° - 2 nesting	RACM-n	ATH-S
WRFNKUA18C	0.17° - 2 nesting	RADM2-n	ATH-S

^a Number of successive nesting to reach the current domain resolution.

^b For the 3 km resolution, three tests with online (feedback of chemistry on meteorology) options: DI (both Direct and Indirect effects), nDI (no Direct, but Indirect effects), DnI (Direct, but no Indirect effects).

^c -n is for the new solver (Rosenbrok) and -o for the initial solver (QSSA) used for WRF-chem.

^d -W refers to the winter episode and -S for the summer episode.

^e A and D WRF-Chem configurations were performed with 4 nested domains, while C and B were run with 3 nested domains only.

Table 4
Model descriptions and main settings.

Model codes	Team name (Country)	Model name and version	Large scale meteo driver and resolution	Emission Inventory, resolution, date	Details on domains and resolution
CHIMCIE	CIEMAT (ES)	IFS-CHIMERE v2017r4	ECMWF/IFS 9 km	EMEP 0.1° and Spanish national inventory, 2015	4 nested domains targeted over Madrid, Paris and Athens: 0.27° , 0.09° , 0.03° , 0.01°
CHIMLMD	LMD/IPSL (FR)	WRF-CHIMERE v2020r1	NCEP/GFS 1.0°	CAMS REG V4.2 0.1° , 2015	3 nested domains over Paris: 30 km, 10 km, 3.3 km
WRFNKUA	NKUA (GR)	WRF-Chem	NCEP/GFS 1.0°	EDGAR HTAP 0.1° , monthly emission distributions, 2010	4 nested domains over Athens: 0.5° , 0.17° , 0.056° , 0.019°

parameterization (Hong et al., 2006) are used. The Morrison double moment scheme for cloud physics (Morrison et al., 2005), and the cumulus parameterization Grell 3D (Grell and Dévényi, 2002) are also implemented. Two gas phase chemistry mechanisms are used, the RADM2 (Stockwell et al., 1990), the RACM (Stockwell et al., 1997) and the aerosol module is MADE/SORGAM (Ackermann et al., 1998). The RACM mechanism, compared to RADM2, considers a more detailed treatment of organic chemistry related to biogenically emitted compounds (monoterpenes). The EDGAR-HTAP (Emissions Database for Global Atmospheric Research-Hemispheric Transport of Air Pollution) global emission inventory is used, including shipping, with a horizontal grid resolution of 0.1° × 0.1° (Janssens-Maenhout et al., 2015) and a reference year of 2010. Biogenic emissions are calculated online with the MEGAN module (Guenther et al., 2006) while initial and boundary conditions for gases and aerosols come from simulations of CAM-chem in CESM2.0 (CESM, 2019). Natural sea salt and soil (online calculation), and biomass burning emissions are also included (Methymaki et al., 2023). For RADM2 chemistry, there are two different solvers available within WRF-Chem. The QSSA (Quasi-steady-state approximation) solver which has been shown to underestimate ozone titration in urban areas with high NO_x emissions (Forkel et al., 2015; Im et al., 2018) and the Rosenbrok solver with adaptive time stepping available in KPP (Kinetic PreProcessor) described in Sandu and Sander (2006), Damian et al. (2002). The A (RADM2), B (RACM) and C (RADM2) configurations use the Rosenbrock solver while the D (RADM2) use the QSSA. The simulated period is split into shorter (3-day) sub-periods

along the episode with a 3 days spin-up. For meteorology, one spin-up day for each sub-period is considered, whereas chemistry runs continuously for the whole period. All simulations were run online considering aerosols-radiation interactions.

WRF-CHIMEREv2020r1 operated by LMD — CHIMLMD

The CHIMERE model is a regional chemistry transport model that can be used in both online and offline configurations in its latest version (Menut et al., 2021; Mailler et al., 2017) for research, future scenarios and operational forecast purposes (Lapere et al., 2021; Bessagnet et al., 2020; Menut et al., 2020). For online modeling, it is coupled with the WRF meteorological model (Skamarock et al., 2008). The model requires a set of gridded data as mandatory input: emission data for both biogenic and anthropogenic sources, land use parameters, boundary and initial conditions, and other optional inputs such as dust and fire emissions. Given these inputs, the model calculates the concentrations and wet/dry deposition fluxes for a list of gaseous and aerosol species (depending on the chosen chemical mechanism). In this study, the model was coupled with WRF using the NCEP (National Centers for Environmental Prediction) input data (NOAA, 2015) for the global meteorological conditions. It was run on a triple nested configuration (one-way nesting), with a coarse domain covering the whole of Europe at a 30 km × 30 km resolution (164 × 165 cells), the intermediate domain with a 10 km × 10 km resolution (45 × 45 cells), while the finest domain focused on the Paris region at a 3 km × 3 km resolution (51 × 52 cells). Over the vertical, 15 layers were used starting from the surface up to 300 hPa. The height of the

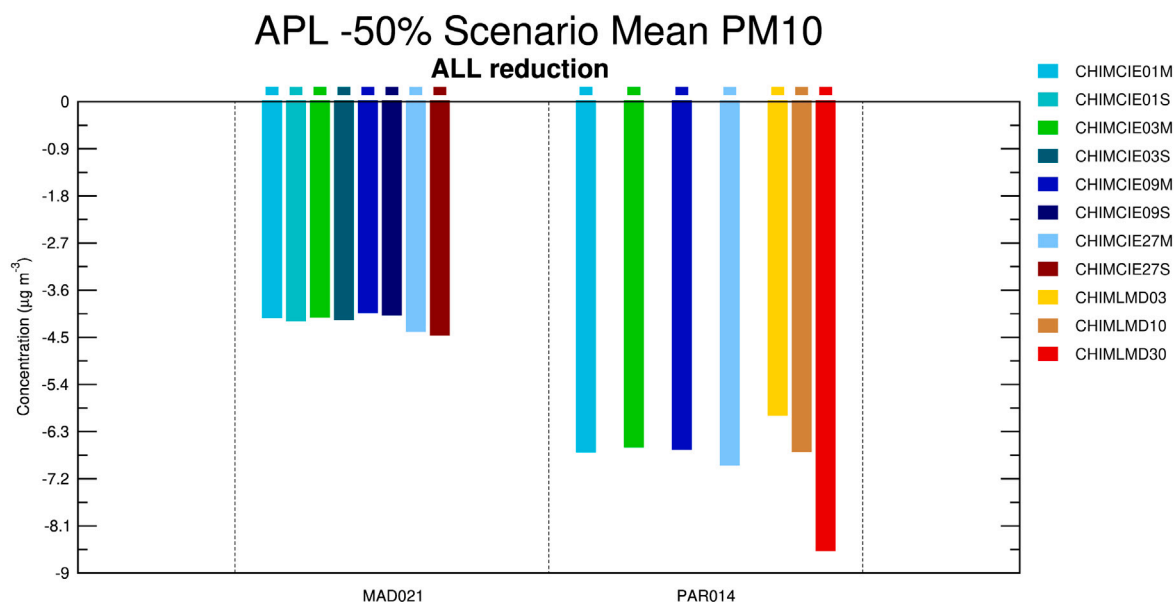


Fig. 2. Impact of 50% emission reductions for ALL precursors pollutants — Absolute Potential APL for mean PM_{10} concentrations averaged over time and the target domains in Madrid and Paris for the winter episode.

first level is 8 m. No fire emissions were used. Boundary conditions were taken from CAMS 3-hourly reanalysis global runs. All major aerosol groups were activated, including elemental carbon, sulfate, nitrate, ammonium, SOA, dust, salt, and PPM; taking into account coagulation, nucleation and condensation processes over 10 size bins ranging between 10 nm and 40 μm . Anthropogenic emissions were prepared using the CAMS regional inventory (Granier et al., 2019) for all simulations. Spectral nudging is applied for all nested domains (also within the planetary boundary layer). The wind components, the potential temperature perturbation and the water vapor mixing ratio are nudged with a relaxation coefficient $g = 0.0003 s^{-1}$. A wave number of 5 and 4 is used, respectively in the x and y directions.

For this exercise, all simulations were run offline without feedback (radiative effects) of aerosols on the meteorology. However, three tests were performed with online (feedback of chemistry on meteorology) options for the base case and the precursor emission reduction by 50% applied to all pollutants together (ALL). Simulations are named CHIMLMD03DI, CHIMLMD03nDI and CHIMLMD03DnI with the suffixes DI (both Direct and Indirect effects), nDI (no Direct, but Indirect effects) and DnI (Direct, but no Indirect effects). Indirect effects refer to the interactions with clouds, whereas direct effects refer to the scattering or absorption of incoming solar radiation by aerosols in the atmosphere. For the former, CHIMERE sends information to the WRF model on the size distribution of aerosol number, the hygroscopic aerosol number size distribution, the aerosol bulk hygroscopicity and the ice nuclei.

IFS-CHIMEREv2017r4 operated by CIEMAT — CHIMCIE

The CHIMERE chemistry transport model v2017 (Mailler et al., 2017) has been extensively used in Europe and, in particular, in Spain Brands et al. (2020), Vivanco et al. (2009). The model requires a set of gridded data as mandatory input: meteorology, emission data for both biogenic and anthropogenic sources, land use parameters, boundary and initial conditions, and other optional inputs such as dust and fire emissions. Given these inputs, the model calculates the concentrations and wet/dry deposition fluxes for a list of gaseous and aerosol species (depending on the chosen chemical mechanism). In this study, meteorological fields were adapted from simulations by the European Centre for Medium-Range Weather Forecasts, ECMWF (www.ecmwf.int); the Integrated Forecasting System (IFS) for 2015, obtained from the MARS archive at ECMWF through the access provided by

AEMET (Agencia Estatal de Meteorología, Spain: www.aemet.es) for research projects Four one-way nested domains were considered for the simulations centered on Madrid, Athens and Paris with horizontal resolutions of 0.27°, 0.09°, 0.03° and 0.01° (approx. 27 km, 9 km, 3 km and 1 km, respectively). In the vertical, 8 layers were used starting from the surface (997 hPa) up to 500 hPa. The height of the first level is 25 m. No fire emissions were used. Boundary conditions for the coarsest resolution domain were taken from LMDZ-INCA and GOCART climatological simulations. All major aerosol groups were activated, including elemental carbon, sulfate, nitrate, ammonium, SOA, dust, salt, and PPM, and taking into account coagulation, nucleation and condensation processes over 10 sizes. Anthropogenic emissions were prepared from the EMEP database at 0.1° x 0.1° spatial resolution (Mareckova et al., 2019). For the Spanish domains the national emission inventory for Spain at the same EMEP grid was used for the Spanish grid squares. The model was run with the MELCHIOR2 (M) and SAPRC07 (S) chemical mechanisms.

3. Results and discussion

Since, (i) the model domains are different (in terms of nesting strategies), and (ii) the target domain where the emissions are reduced are the same, we chose for the sake of coherence this target domain as a common domain for the spatial comparisons (either using median, mean or percentile values) of concentrations and for displaying maps. In this study, we only analyze the impact of the 50% reduction. All model outputs for a given city are bi-linearly interpolated over the target domain as defined in Table 1 at a 0.01° resolution.

After an analysis of the impact of the various configurations (mainly focusing on the impact of the chemistry scheme) on time averaged indicators for PM and Ozone (Section 3.1), the analysis will focus afterwards on the impact horizontal resolution (Section 3.2). An analysis on hourly values of indicators is then provided (Section 3.3). From the outcomes of the last sub-sections come to a discussion on the effect of activating online coupling on model responses (Section 3.4).

3.1. Overall variability of model responses

3.1.1. Particulate matter as PM_{10}

Regarding the impact of emission reductions on PM_{10} concentrations (Fig. 2) considering a reduction of all precursors together over

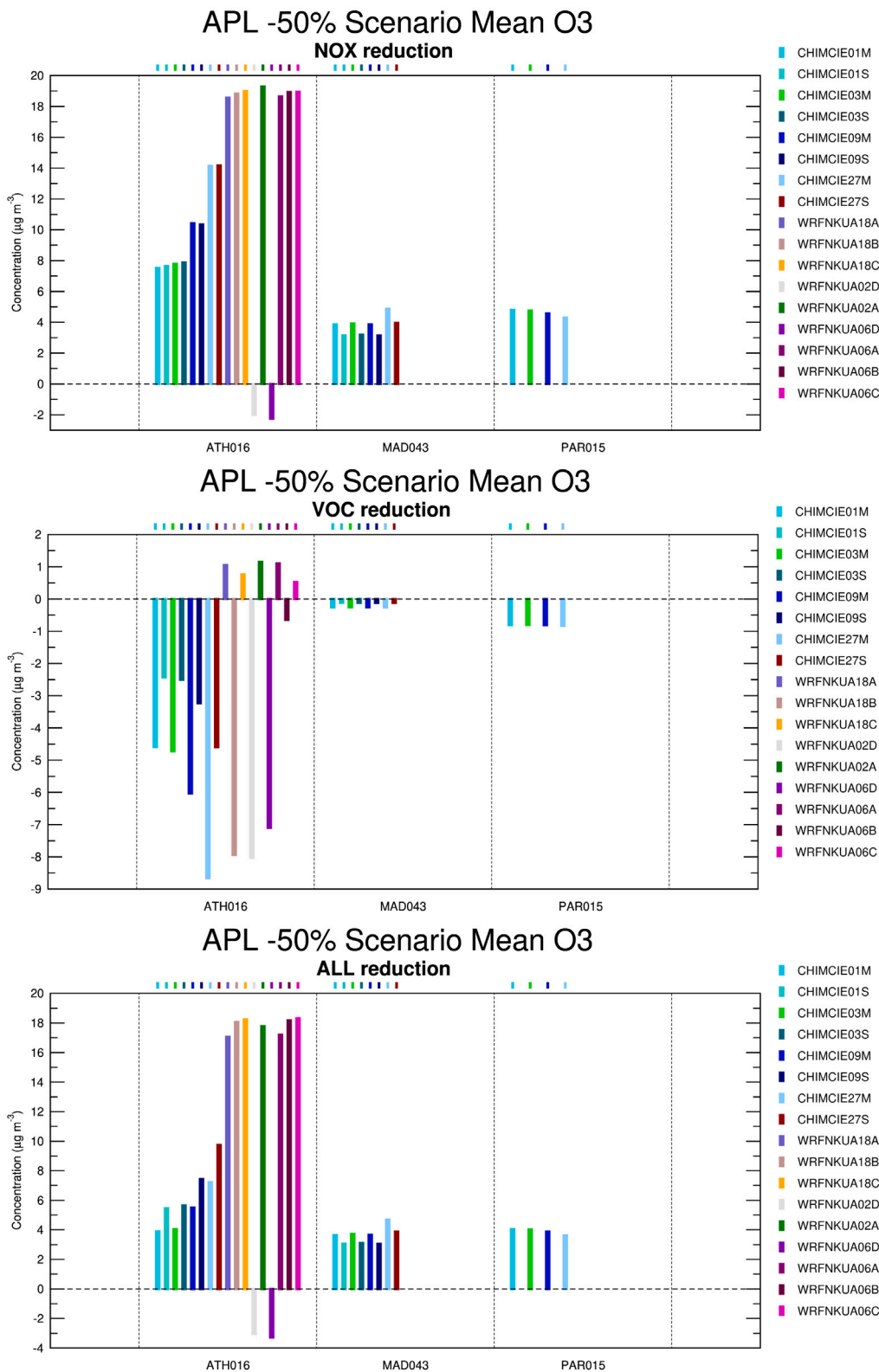


Fig. 3. Impact of 50% emission reductions (NO_x, VOC and ALL together) - Absolute Potential APL for mean Ozone concentrations averaged over time and the target domain.

APY -50% Scenario Mean NO2

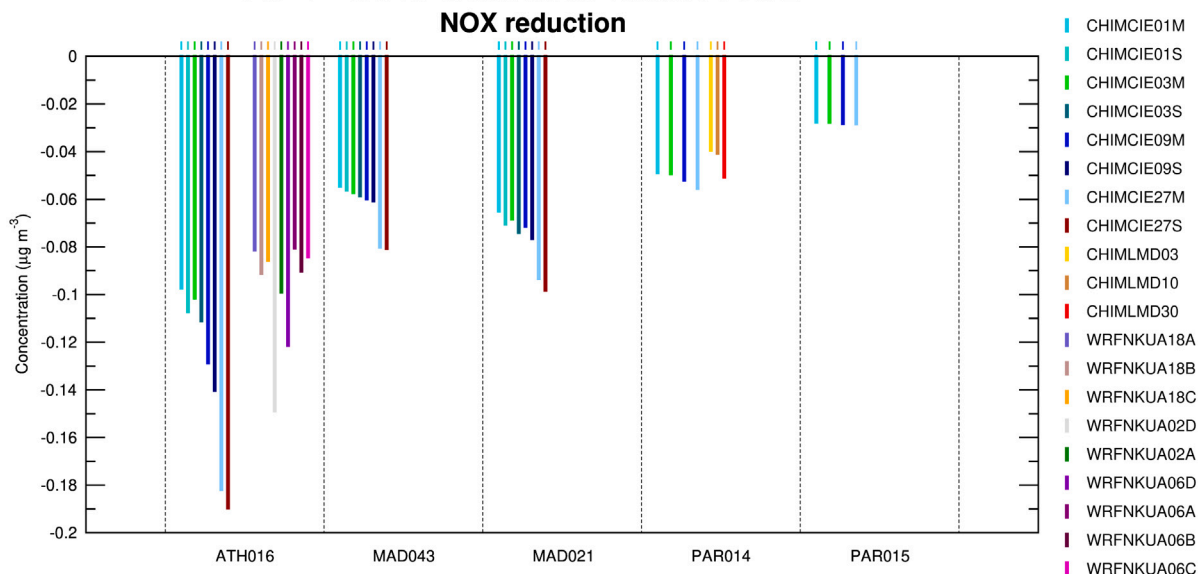


Fig. 4. Impact of 50% emission reductions for winter and summer episodes for a NO_x emission reduction — Absolute Potency APY in µg m⁻³ per ton of abated emissions for mean NO₂ concentrations averaged over time and the target domains.

Table 5

Average over time and space of the Relative Potential (RPL) in % for some episodes focusing on PM compounds and precursors or associated gases (dark blue for RPL < -30%, dark green for -30% ≤ RPL < -10%, light green for -10% ≤ RPL < -5%, light blue for -5% ≤ RPL < -0.1%, yellow for -0.1% ≤ RPL < 0.1%, orange for 0.1% ≤ RPL < 100% and violet for RPL > 100%).

Model configuration	Scenario -50%	PM ₁₀	SO ₄	SO ₂	NH ₄	NH ₃	NO ₃	HNO ₃	NO ₂	Gratio
PAR014 - Winter										
CHIMLMD03	PPM	-15.0	-0.0	+4.4	-0.2	+0.6	-0.3	-1.9	-5.9	+0.2
	SO _x	-2.6	-5.4	-84.3	-0.2	+3.3	+1.0	-3.8	-6.3	+1.9
	NH ₃	-10.5	-2.1	+7.4	-12.7	-66.4	-14.0	+45.6	-4.7	-23.0
	NO _x	-5.2	+2.2	+2.9	-3.9	+13.6	-5.8	-35.9	-68.2	+7.2
	VOC	-2.9	-0.4	+4.6	-0.0	+0.2	0.0	-9.1	-8.4	+0.4
	ALL	-23.8	-6.1	-86.6	-15.2	-55.8	-16.9	-6.3	-63.9	-15.0
CHIMCIE03M	PPM	-14.7	+0.1	-0.1	-0.4	+0.3	-0.5	-0.9	+0.2	+1.2
	SO _x	-2.0	-18.0	-68.0	-2.5	+2.5	+0.3	-5.1	+0.3	+2.5
	NH ₃	-5.2	-10.5	+19.2	-11.6	-84.8	-7.3	+117.4	0.1	-57.3
	NO _x	-0.8	+0.8	-1.4	-1.5	+1.3	-2.7	-9.6	-60.7	+8.7
	VOC	-1.0	+0.2	-0.3	-1.1	+0.8	-1.6	-3.7	-1.4	+0.7
	ALL	-22.9	-23.0	-59.1	-15.5	-81.3	-10.9	+79.9	-61.4	-48.3
MAD021 - Winter										
CHIMCIE03M	PPM	-28.5	+0.2	-0.3	-1.3	+0.7	-4.0	-0.8	+0.3	+1.7
	SO _x	-1.1	-9.2	-107.4	-3.4	+9.4	+3.6	-5.7	+0.0	+7.3
	NH ₃	-8.6	-23.6	+19.5	-28.6	-74.4	-39.9	+50.2	+0.1	-59.5
	NO _x	-0.8	+1.6	-0.7	-3.0	+2.8	-10.4	-9.1	-72.6	+9.7
	VOC	-0.3	+0.1	-0.1	-0.4	+0.4	-1.1	-1.6	-0.0	+0.6
	ALL	-38.2	-28.6	-95.1	-33.5	-66.2	-45.7	+26.7	-72.3	-46.1
ATH016 - Summer										
WRFNKUA6B	NO _x	-0.9	-4.6	-2.1	-6.8	+0.7	-1.1	-14.1	-77.6	+10.5
	VOC	-0.9	-1.6	+1.0	-2.8	+2.0	-10.2	+0.5	-0.3	+6.5
	ALL	-1.2	+0.2	-0.2	-0.4	-2.9	-10.1	-11.7	-75.7	+2.1

Paris and Madrid for the winter episode (and by precursors in supplementary file C), it is clear that PPM emission reductions drive the concentration delta, leading to substantial decreases. In Paris, the delta is higher than for Madrid even when we look at the RPL reducing PPM only (not shown here) which is normalized by the PM₁₀ concentrations of the base case. SO_x, VOC and NO_x emission reductions produce the lowest impact usually below 0.5 µg m⁻³. Even where NH₃ emissions are low, as in urban areas, reductions of NH₃ have large impacts because of the chemical regime, NH₃ controlling the impact. On average, CHIMERE simulations run by LMD have a delta close to zero for SO_x emission reductions.

The chemistry scheme has a low impact on the PM₁₀ APL, in general, although the PM₁₀ deltas are more negative for NO_x and SO_x emission reductions and slightly less negative for VOC reductions with MELCHIOR than with the SAPRC scheme in Madrid. Table 5 displays the change of all PM components (through their RPL) and their precursor or associated gases like nitric acid, ammonia and sulfur dioxide when reducing emissions by 50%. Reducing only PPM emissions can affect all gases and compounds, indeed the heterogeneous chemistry is affected as well as the gas-partitioning of inorganic species. When ammonia emissions are reduced, average nitric acid concentrations can largely increase over the episode. There is a clear difference between

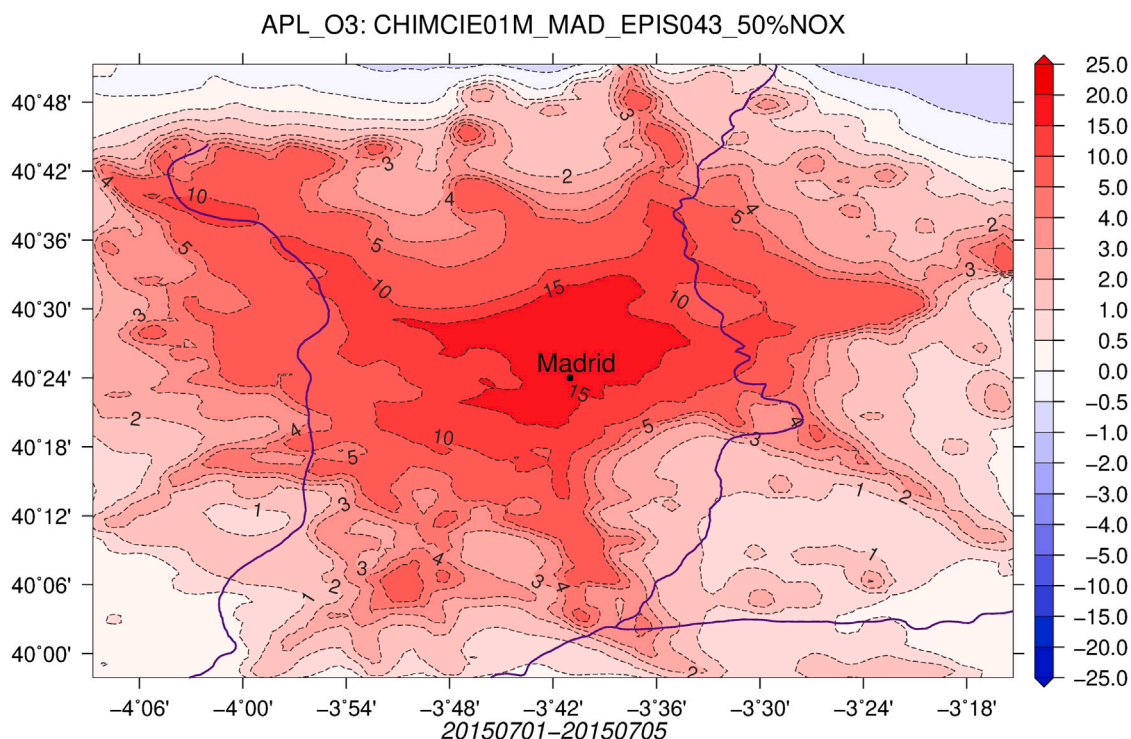


Fig. 5. Spatial patterns of impact of 50% NO_x emission reductions for emission reduction scenarios and model configurations over Madrid. Absolute Potential APL for O_3 mean concentrations averaged over time.

CHIMLMD and CHIMCIE over Paris (Table 6), in that the *Gratio* is always above 1 for CHIMERE run by the CIEMAT, even for the lowest percentiles, leading to a small impact of ammonia emission reductions. In the case of CHIMERE run by LMD, the decrease of ammonia emissions is more efficient since there are many locations in the domain where the *Gratio* < 1, particularly over the most urbanized areas.

The linearity ratio in supplementary file B consistently shows on average an increase of efficiency when passing from a 25% to a 50% NO_x and NH_3 emission reductions, even if this efficiency is lower over Paris for ammonia than for NO_x because ammonia is clearly in excess for this area, according to the value of the *Gratio*. As shown in Table 6, the *Gratio* is much lower for CHIMERE run by the LMD due to the ammonia emission inventory which has values 3 times lower over Paris compared with the CHIMERE configuration run by CIEMAT. Therefore, the sensitivity to an ammonia emission reduction is much higher in the CHIMLMD simulations than in the CHIMCIE simulations. We observe a perfect linearity when PPM emissions are reduced when comparing -25% and -50% emission reductions (deviation to linearity ratio close to 0 in supplementary file B). This highlights that PPM concentrations are mainly driven by linear processing, very weakly by indirect effects of physico-chemical processes.

For the CHIMERE simulations over Madrid, it is noteworthy that a reduction of SO_x emissions by 50% can lead, on average, to a reduction of more than 50% of SO_2 concentrations (e.g. RPL about -107%). Since the production of sulfates by aqueous chemistry is influenced by pH, the production of sulfate is enhanced when the pH increases, leading to less sulfur in the gaseous phase. For the summer episode in Athens, we show that for the WRF-Chem model the emission reductions of VOC and NO_x have a very weak influence on the PM_{10} concentrations which is attributed to the significant fraction of the natural coarse aerosols in PM_{10} concentrations in this coastal region. However, nitric acid and nitrate are also affected. This confirms the central role of nitric acid species involved in gaseous chemistry and also in gas-to-particle conversion processes that are very sensitive to meteorological parameters and concentration. The *Gratio* is very low for the summer

episode in Athens and even negative for the lowest percentiles due to the low ammonia emissions in this region at this time of the year.

The maps of APL over the three target domains in Paris, Madrid and Athens are displayed in supplementary file C. Over Paris, the APL for an emission reduction of 50% for all precursors is negative everywhere with the largest concentration decrease in the very center of the domain, reaching $-20 \mu\text{g m}^{-3}$. CHIMERE operated by CIEMAT and LMD under different configurations display similar spatial patterns of APL for the Paris episode.

3.1.2. Ozone and nitrogen dioxide

In urban VOC-limited areas (Fig. 3), the expected behavior for ozone is an increase for NO_x emission reductions and a decrease for VOC emission reductions. Usually, the magnitude of this response is larger for the NO_x reduction and dominates the response for a combined NO_x -VOC emission reduction. In Athens, for the CHIMERE simulations the negative delta with the MELCHIOR scheme is double that for SAPRC (Fig. 3). The delta for WRF-Chem B (RACM) configuration is similar to CHIMERE for coarser resolutions, however this behavior is not retained for the high resolution simulations and for the C (RADM2) configuration. Differences in the treatment of organic chemistry between the two schemes in relation with the large magnitude of NO_x emissions may even change the sign of the delta. This is also supported from the VOC/ NO_x ratios (Table 7); the B (RACM) configuration ends in larger ratios compared to the C (RADM2) case. Some WRF configurations (like WRFNKUAD) lead to small negative deltas for NO_x reductions and to an increase for VOC emission reductions. This latter behavior is surprising and impossible to explain only by chemistry (Carter et al., 1982), Section 3.4 will provide an explanation with the involvement of online effects.

As displayed in Table 7, WRF-chem and CHIMERE simulate very different ozone formation regimes over Athens. WRF-chem estimates a VOC-limited regime most of the time whereas CHIMERE estimates a VOC-limited regime where NO_x emissions are the highest and NO_x -limited over less urbanized areas. The simulations WRFNKUA2 A and WRFNKUA2D allow the testing of two different chemical solvers while

keeping the same set-up for all other parameters. The APL for ozone has a different sign for NO_x emission reductions. For instance, reducing NO_x with the Rosenbrok solver leads to an APL of 19 μg m⁻³ whereas it is close to -3 μg m⁻³ with the QSSA solver. This is likely explained by QSSA shortcomings that are documented in the literature, as well as to some underestimation of ozone titration in urban areas with high NO_x emissions that have also been reported (Forkel et al., 2015). It is noteworthy to mention such a sensitivity on a response to an emission change with a numerical setting.

As shown in supplementary file C and Fig. 5 focusing on Madrid, the difference between the APLs for NO_x and VOC emission reductions over Madrid is large. For the NO_x case, there is a positive delta (titration effect) within the urban areas and a slight increase close to the north borders of the domain. For VOC there is a small decrease everywhere. Over Athens, WRF-chem run by NKUA estimates a very large increase in ozone for NO_x emission reductions (about +25 μg m⁻³). For VOC emission reductions, the spatial patterns over Athens shows a general decrease of concentrations over the land except in the north of Athens and some positive APL values over the seas reaching 3 μg m⁻³. These patterns are shaped by the different meteorological conditions during the simulated period, strong northeastern winds during the first days and then sea breeze conditions with winds from the southern sector.

The strong increase of ozone when reducing NO_x emissions is mainly due to the particular chemical regime resulting from the WRF-Chem configurations in Athens with an emission dataset with very high NO_x emissions (about 100 mg m⁻²day⁻¹) compared with the CHIMERE set-up by CIEMAT (about 40 mg m⁻²day⁻¹) and very low anthropogenic VOC emissions, 2 to 3 times lower than the emissions used for CHIMERE. This difference in emissions explains the factor of 5 difference for the VOC/NO_x ratio in Table 7 in Athens. As shown in supplementary file B, over Madrid and Paris, emission reductions generally lead to near linear responses, although there is a clear decrease in APL between 25% to 50%.

The results for NO₂ is analyzed in Fig. 4 and supplementary file C, focusing on the absolute potency APY. For this pollutant, we have voluntarily moved to the APY indicator because this pollutant will be more sensitive to local NO_x emission reductions. NO₂ is not affected much by PPM and SO_x emission reductions. Obviously, the NO_x emission reduction provides the highest negative potency. The PPM emission reduction scenario for all model configurations increases NO₂ concentrations slightly. Since MELCHIOR accounts for heterogeneous reactions that destroy nitrogen oxides on particle surfaces, reducing the amount of particles reduces the efficiency of these reactions and, therefore, NO₂ concentrations increase slightly. These heterogeneous chemistry effects are well documented and can impact the full chain of gaseous reactions involving nitrogen species up to ozone concentrations (Chan et al., 2021; Li et al., 2019).

3.2. Impact of the horizontal resolution

As shown in Fig. 2, the resolution has a low impact on the PM₁₀ APL. For PM₁₀, while for CHIMLMD some variability is observed in Paris considering the various resolutions, the RPL is quite constant around of -26% for the 3 resolutions CHIMLMD03, CHIMLMD10 and CHIMLMD30.

Regarding Ozone in Athens and for the high-resolution domains, the concentrations increase for the WRFNKUA simulations and is almost double than that of the CHIMCIE simulations which is attributed to the higher magnitude of NO_x emissions in this urban area considered by the WRFNKUA system. The differences between the two modeling systems reduce in coarser resolutions for the Athens case. The impact of resolution in CHIMCIE simulations is lower for Madrid and Paris compared to Athens (Fig. 3).

As for ozone concentrations simulated by WRFNKUA in Athens during the summer episode, the NO₂ APY changes sign when reducing VOC emissions between the 18 km resolution to the 6 km resolution,

Table 6

Base case *Gratio* percentiles over the domains for some model configurations computed over all hourly and grid cell values for some episodes.

Model	10th	25th	50th	75th	90th
PAR014 - Winter					
CHIMLMD03	+0.76	+0.87	+1.06	+1.30	+1.81
CHIMCIE01M	+1.16	+1.39	+1.87	+3.09	+6.05
CHIMCIE03M	+1.16	+1.39	+1.86	+3.05	+6.00
MAD021 - Winter					
CHIMCIE01M	+0.85	+1.47	+2.22	+3.41	+5.09
CHIMCIE03M	+0.87	+1.44	+2.15	+3.29	+4.92
ATH016 - Summer					
WRFNKUA6B	-0.09	+0.03	+0.20	+0.57	+1.19
WRFNKUA6C	-0.62	-0.14	+0.10	+0.46	+1.06

Table 7

Base case VOC/NO_x ratio percentiles over the domains for some model configurations computed over all hourly and grid cell values for some episodes.

Model	10th	25th	50th	75th	90th
PAR015 - Summer					
CHIMCIE01M	3.43	4.48	5.87	8.27	12.54
CHIMCIE03M	3.46	4.48	5.76	8.19	12.29
MAD043 - Summer					
CHIMCIE01M	4.12	6.89	12.59	26.73	51.01
CHIMCIE03M	4.17	6.80	11.98	25.61	48.20
ATH016 - Summer					
CHIMCIE01M	4.84	7.92	12.99	24.48	45.73
CHIMCIE03M	5.09	8.16	13.13	23.77	42.81
WRFNKUA6B	0.90	1.10	2.20	5.27	14.45
WRFNKUA6C	0.92	1.10	2.00	4.63	13.39

with a different order of magnitude. Even if the APY is low, this impact remains at this stage difficult to explain, although Section 3.4 provides a plausible explanation. For the other winter and summer episodes, the change of configuration (resolution as well as chemistry schemes) of CHIMERE is more in line with what is expected *i.e.* a limited impact of resolution with very low absolute values.

An increase in resolution has an important impact on NO₂ concentrations, increasing deltas at higher resolutions. Interactions between VOC and NO_x on the formation of ozone lead to some visible effects of the resolution on NO₂ potency. There is a noticeable impact of the spatial resolution on NO₂ concentrations for NH₃ emission reductions on the potency with CHIMERE run by LMD over Paris, with an increase of the APY when reducing the resolution from 3 to 30 km.

3.3. Impact of chemistry on hourly air pollutant concentrations

In this section, we focus our analysis on hourly timeseries of APL. The impact of the chemistry schemes on the hourly APL is shown in Fig. 6 and supplementary file C for the ozone episodes. The light blue and red dashed curves represent the timeseries of the median APL (over space) either for ozone or nitric acid (HNO₃), the APL being calculated for either a 50% reduction in VOC or NO_x emissions correspondingly. The black curve is the delta of APL (ΔAPL) for both configurations *i.e.* the difference between the light blue and red curves.

With regards to the differences between SAPRC (S) and MELCHIOR (M) with CHIMERE for Athens, reducing NO_x emissions by 50% has a low impact of the ΔAPL at the beginning of the episode (strong northeastern winds). When ozone concentrations starts to increase in the second period of the episode, with a more pronounced diurnal cycle (sea breeze conditions), the influence of the chemistry can be mainly observed during the morning. These fluctuations are correlated with a global increase of nitric acid fluctuations. However, daytime ozone APL is less affected by the chemistry scheme. This behavior is also observed in Madrid.

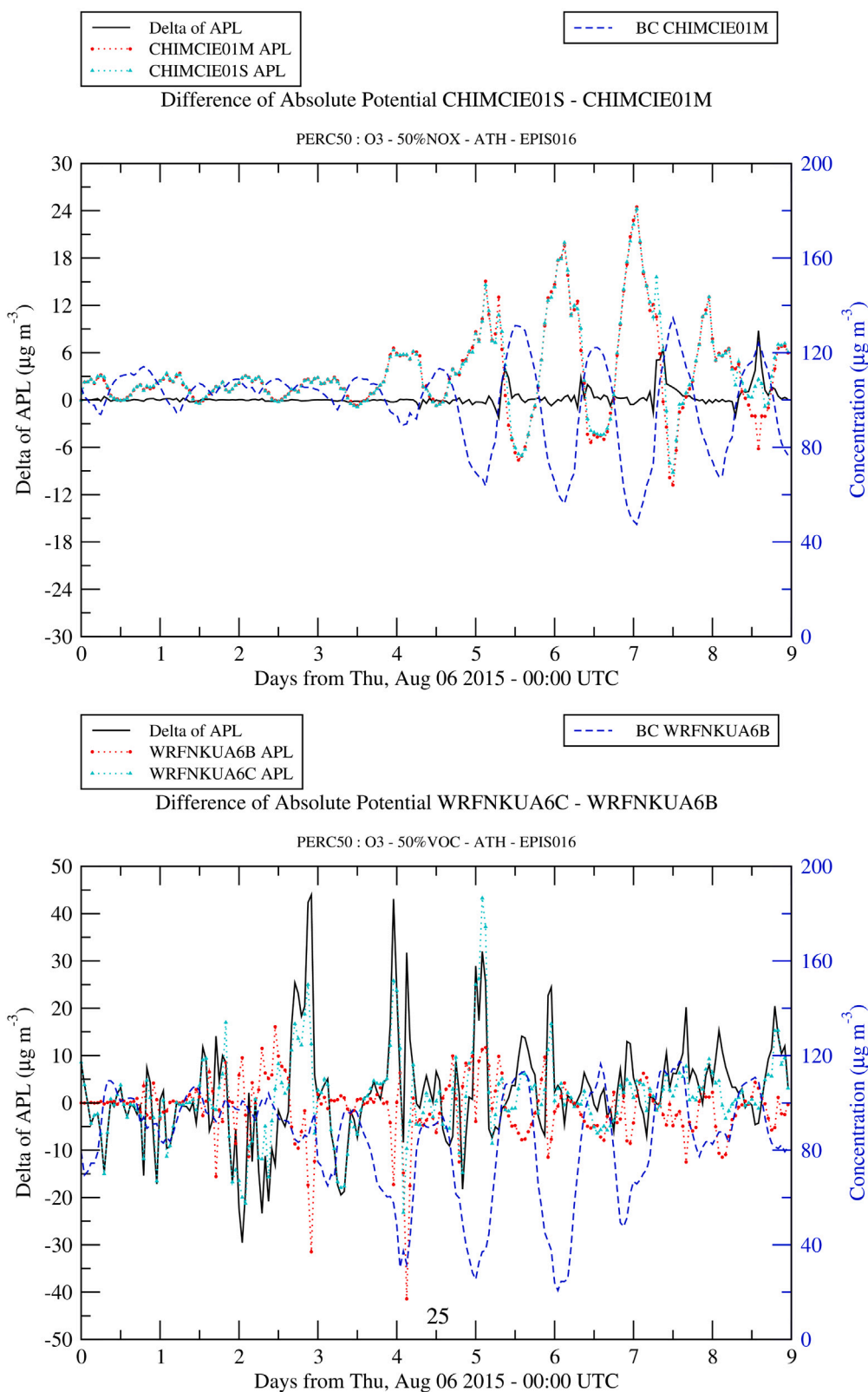


Fig. 6. Evolution of the ozone delta of APL (reducing VOC and NO_x) comparing a modification of the chemical scheme, over Athens for a summer episodes. The light blue and red curves represent the APL for each configuration while the solid black line is the difference between the two curves. The blue dashed line is the base case concentration of one of the configurations.

By contrast, the difference in the APL for both ozone and nitric acid due to chemistry (RADM2 vs. RACM) in the WRF-Chem simulations over Athens is more variable throughout the period. For these

simulations, the largest differences in APL between the RADM2 and RACM chemistry schemes occur around 12:00 UTC and are associated with the more detailed organic chemistry of biogenic emissions in

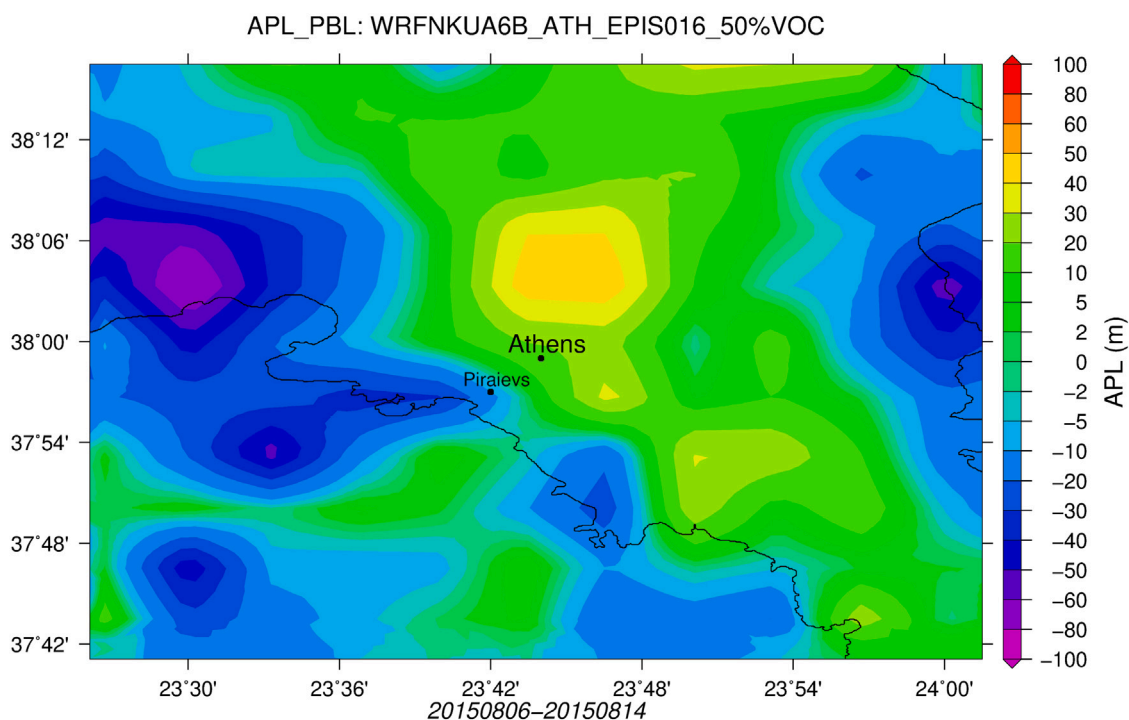


Fig. 7. Time-averaged APL of the planetary boundary layer height (PBL in m) over the episode when reducing VOC emissions by 50% with the WRFNKUA6B configuration. A mean APL of 50 m (delta of about 25 m) of the PBL is observed close to Athens.

RACM scheme. The ΔAPL can sometimes exceed $20 \mu\text{g m}^{-3}$ for ozone concentrations. Differences also occur at night associated with the titration effect.

The different impact on chemistry schemes in the same region is related with differences in VOC/ NO_x ratios (Table 7) which in turn reflect emissions differences such as anthropogenic emissions magnitude, and/or inclusion of non-anthropogenic emission sources (biogenic, biomass burning). The different processes used to derive meteorological fields in the two modeling system is also crucial (Russell, 2000); large scale based for CHIMERE, prognostic mode for WRF-Chem. In WRF-Chem the variability of APL reflects both the online coupling of meteorology-chemistry simulations (run in parallel at every time step) as well as the feedbacks of chemistry on meteorology. This variability reflects a corresponding variability of the meteorological fields (e.g. PBL height). The simulation of ozone episodes and peak concentrations during sea breeze conditions in the greater Athens depend critically on several factors including the biogenic emissions, meteorology and ozone background levels (Bossioli et al., 2007). The latter one is crucial at the peripheral stations (northern part of the basin), during the morning and night hours. On an hourly basis, there is no particular impact of the chemistry scheme MELCHIOR or SAPRC on PM_{10} concentrations (not shown here) for the simulations over Madrid.

3.4. Impact of online coupling

An issue is raised from two main outcomes from the previous analysis particularly when looking at VOC emission reductions over Athens: (i) the erratic behavior of ozone responses to anthropogenic emission reductions when changing the chemical scheme, and (ii) the fact that reducing VOC emissions could lead, for some configurations of WRF-Chem to increase ozone concentrations. Actually, WRF-Chem is run online (meteorology-chemistry run in parallel at every time step) and with a full feedback of the different air pollutants on the meteorology through the direct and indirect impacts of aerosols on the radiative budget. This means that a change of emissions implies a change in PM concentrations which in turn modify the radiative budget, and thus the whole meteorology.

Fig. 7 shows clearly how the planetary boundary layer (PBL) height is affected by a change of emissions. Close to Athens, an absolute potential of 50 m for the PBL is observed, on average over the period. Afternoon PBL heights in the region during the simulation period vary between 400 m and 2000 m. These feedback processes have been observed in previous studies (Bessagnet et al., 2020; Cholakian et al., 2023; Menut et al., 2019) with CHIMERE coupled online with WRF. Precipitation and cloud formation are obviously affected by these feedback since very small variations greatly affect threshold-influenced processes. The validation of these feedback in online models remains a challenge, they can be conducted by comparing pollutant concentrations against observations considering or not feedback, or in a better way by evaluating the ability of the radiative module to diagnose the radiative fluxes or other related variable along the modeling chain Aouizerats et al. (2010), Baklanov et al. (2014). As reminded in Baklanov et al. (2017), meteorological models are tuned to run well without feedbacks (by using aerosol climatologies), leaving room for improving the modeling abilities.

Another important setting that can play a role is “nudging”. Nudging is used over a limited area, the regional model will be driven at its boundaries by a global model. Within the domain, the same relaxing from the large scale can be done with the technique of nudging. Nudging is a data assimilation technique that was created to avoid divergences (Kruse et al., 2022) and ensure that the model follows a large scale predefined trajectory. However, this dampening technique is also a limitation to our understanding of processes by inhibiting the modeling of the physics.

The use of nudging in models has shown its usefulness for many applications. For example, a study (Otte et al., 2012) showed that for regional meteorology, nudging could preserve both averages and extremes of meteorological variables like the temperature. But they cite several studies showing that the nudging (including the spectral nudging) weakened the extreme meteorological events observed such as tropical cyclones. A hard nudging of the large scale fields is equivalent to a smart interpolator on a finer grid, while a soft nudging lets the model develop its own physics within the domain only taking into account large scale effects at the boundaries.

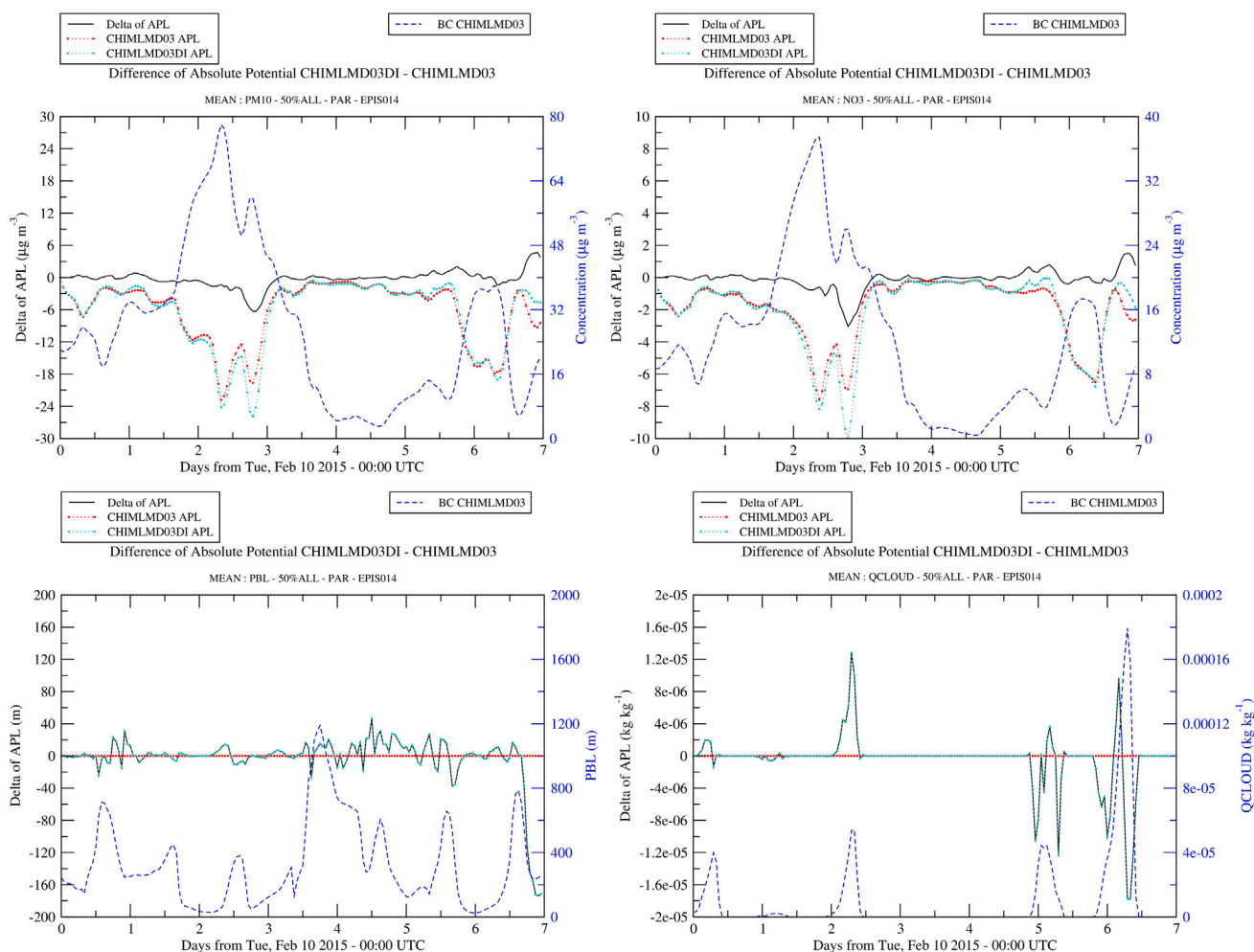


Fig. 8. Time series of mean impact (APL) over Paris to analyze the effect of the full online coupling (Direct and Indirect effects) for scenario 50%ALL. The APL is computed for PM_{10} , Nitrate concentrations (top) and two meteorological variables (bottom): the Planetary Boundary Layer height and the cloud water content QCLOUD at the first level. The delta of APL (solid line black curve) between both configurations (offline versus online) is then the difference between the light blue and red dashed curves. The dashed blue line is the time series of the base case of one of the configuration.

In our study, WRF-Chem used over Athens is not nudged. The meteorological fields are predicted (in 3-days sub-periods) and not relaxed by the large scale fields. Any additional perturbations of the meteorology related to the change of emissions is also not relaxed. Therefore, the positive APL for ozone can be explained by both (i) the absence of nudging, and (ii) the activation of all feedback.

For the winter episode in Paris, we added settings to the base case and to the “all precursors” scenario to test several options: (1) no feedback with aerosols (normal Base case), (2) no direct but indirect effects (nDI), (3) direct but no indirect effect (DnI) and (4) both direct and indirect effects (DI). With these set-ups we can properly analyze the effect of the feedback on the APL. CHIMERE fully coupled with WRF is configured with default spectral nudging so that the model is relaxed with the large scale GFS meteorological data to avoid drifting within the domains. In Fig. 8, the time series of APL for some variables during the Paris episode are displayed. For the PBL and the cloud water content (QCLOUD in WRF) the APL when reducing the emissions by 50% is equal to zero when considering no feedback of the aerosols on the meteorology (red curves).

Therefore, the APL and the ΔAPL are the same (light blue and black curves) showing the impact of the online configuration on the meteorological variable. An APL of ± 20 m for the PBL, on average, is observed

during the episode with a drop of more than 200 m at the end showing a significant impact of the online processes on the meteorology. The cloud water content is also affected, this variable is key because it can lead to the formation of clouds, which can greatly affect the radiative budget and, therefore, the whole meteorology and the related gas and aerosol chemistry. Indeed, SO_2 emissions are transformed into sulfate concentrations due to the oxidation of SO_2 by H_2O_2 and O_3 in clouds, this is a very important mechanism for sulfate aerosol production.

As a consequence, the APL for PM_{10} (and nitrate) is affected by these online effects leading generally to a decrease of the APL by up to $5 \mu g m^{-3}$, which represents about 20% of the APL for PM_{10} . Looking at the indirect and direct effects on the PM_{10} APL (supplementary file B), there are no cumulative effects which was expected with such non linear processes. For instance, during the last day of the Paris winter episode, while the accumulated delta APL in the morning is close to $+15 \mu g m^{-3}$, the simulation with both effects leads to a delta of APL close to 0. This shows the very complex behavior of these feedback, which cannot be disentangled easily.

On 12 February in the morning, the positive APL of QCLOUD at ground level means that foggy conditions are enhanced, on average, by emission reductions, leading to an increase in the PBL that, in turn, leads to a larger reduction in concentrations (*i.e.* a more negative APL

for PM₁₀). Note that the WRF-CHIMERE model by LMD has a less stochastic behavior than the WRF-chem simulation, most likely related to the spectral nudging which guides the model and avoids diverging from the large scale meteorology. A shortcoming of nudging is that this technique tends to dampen the effect of aerosols on the meteorology (Baklanov et al., 2017). This technique must be carefully tested before launching a series of simulations to appropriately calibrate the nudging (relaxation coefficients), as discussed in He et al. (2017).

4. Conclusions

This in-depth analysis of the influence of particular model settings on model responses to emission changes focuses on the impact of the spatial resolution and the chemistry schemes. The results regarding the influence of the chemical schemes used in the models highlight some unexpected behaviors related to the use of online models. From this analysis, the following conclusions can be drawn:

- The spatial resolution has a low impact on the model responses, a resolution of 3 km is probably sufficient to assess emission reduction plans both for Ozone and PM in medium to large urban areas. For NO₂, the impact of the resolution is larger in case of NO_x emissions reductions, with larger responses for finer resolutions.
- The choice of the chemistry scheme has more impact on hourly time series of indicators than for time-averaged values, particularly at night for the ozone chemistry. Related to this, the chemical solver also has a large impact on model responses.
- For secondary species, the chemical regime is of major importance to understand the model response to an emission change. Thus, reducing an emitted species (like NH₃), which is not 'limiting', could have a small or no impact.
- The process to derive the meteorological fields (nudging, reanalysis, forecasting mode) for the air quality simulations is crucial.
- The use or not of direct and indirect effects of aerosol on the radiative budget has a significant effect on model responses.
- With regards to the latter point, it was shown that activating online effects (in coupled meteorology-air quality models) provides an indirect way to analyze the effect of the meteorology on model responses. This is very important, particularly through cloud formation (fog at ground levels), potentially leading to large changes in the PBL, temperature and in cascade, consequently, in all meteorological variables.

This study informs the air quality modeling community on what extent some model settings can affect the expected model responses to emission changes. We suggest to not activate online effects when analyzing the effect of an emission reduction strategy to avoid any confusion in the interpretation of results even if an online simulation should represent better the reality. Other settings related to the emission injection heights or the vertical extent or resolution would also be worth investigating in the future.

CRedit authorship contribution statement

Bertrand Bessagnet: Writing – review & editing, Writing – original draft, Validation, Formal analysis, Data curation, Conceptualization. **Elissavet Bossioli:** Writing – review & editing, Methodology, Formal analysis, Data curation. **Arineh Cholakian:** Writing – review & editing, Methodology, Formal analysis, Data curation. **Marta García Vivanco:** Writing – review & editing, Methodology, Formal analysis, Data curation. **Kees Cuvelier:** Writing – review & editing, Methodology, Formal analysis, Data curation. **Mark R. Theobald:** Writing – review & editing, Methodology, Formal analysis, Data curation. **Victoria Gil:** Writing – review & editing, Methodology, Formal analysis, Data curation. **Laurent Menut:** Writing – review & editing, Methodology, Formal analysis, Data curation. **Alexander de Meij:** Writing –

review & editing, Methodology, Formal analysis, Data curation. **Enrico Pisoni:** Writing – review & editing, Supervision, Project administration. **Philippe Thunis:** Writing – review & editing, Supervision, Project administration.

Declaration of competing interest

The authors declare that they have no known competing financial interests or personal relationships that could have appeared to influence the work reported in this paper.

Data availability

Data will be made available on request.

Acknowledgments

CIEMAT acknowledges the Ministry for the Ecological Transition and Demographic Challenge for financial support. CIEMAT is also grateful for the services offered by the European Center for Medium-Range Weather Forecasts (ECMWF), including the provision of meteorological modeling data with thanks also to AEMET for managing access to this information. The WRF-Chem NKUA simulations were supported by computational time granted from the National Infrastructures for Research and Technology S.A. (GRNET S.A.) in the National HPC facility – ARIS –. For LMD, the work was granted access to the HPC resources of TGCC under the allocation 2021- GEN10274 made by GENCI.

Appendix A. Linearity and additivity ratio

As described in Bessagnet et al. (2023), the 25% and 50% emission reductions are used to calculate a ratio (%) of deviation to linearity (or simply Linearity) defined in Eq. (A.1) for a precursor emission reduction:

$$Linearity = 100 \times \left(\frac{APL_{50\%}}{APL_{25\%}} - 1 \right) \quad (A.1)$$

- $Linearity > 0$: the decrease or increase is amplified from 25% to 50% reduction,
- $Linearity = 0$: the 25% and 50% related increases or decreases are equal, the linearity is perfect,
- $-100\% < Linearity < 0$: the decrease or increase is reduced from 25% to 50% emission reduction,
- $Linearity \leq -100\%$: the sign of impact changes from 25% to a 50% emission reduction.

The available scenarios also allow the analysis of the additivity property, by comparing the sum of individual precursor (m) emission reductions (50%) applied separately called "ADD" ($\sum_m APL_m$) with the combined reduction of precursor emissions called "ALL". Here, we test this property on the absolute potential. The following criteria called "deviation to additivity" in % (or simply Additivity) is defined in Eq. (A.2):

$$Additivity = 100 \times \left(\frac{APL_{ALL}}{APL_{ADD}} - 1 \right) \quad (A.2)$$

- $Additivity > 0$: the decrease or increase is amplified from ADD to ALL emission reduction,
- $Additivity = 0$: the ALL and ADD related increases or decreases are equal, the additivity is perfect,
- $-100\% < Additivity < 0$: the decrease or increase is reduced from ADD to ALL emission reduction,
- $Additivity \leq -100\%$: the sign of impact changes from ADD to a ALL emission reduction.

Appendix B. Supplementary material

- Supplementary file A : evaluation of all base case simulation against available observations
- Supplementary file B : additional figures to support the analysis
- Supplementary file C : extra figures to extend the analysis of Figs. 2,4, 5, 6
- Supplementary file D : additional figures showing the differences between emission inventories

Supplementary material related to this article can be found online at <https://doi.org/10.1016/j.envres.2024.119112>.

References

- Ackermann, I.J., Hass, H., Memmesheimer, M., Ebel, A., Binkowski, F.S., Shankar, U., 1998. Modal aerosol dynamics model for Europe. *Atmos. Environ.* (1994) 32 (17), 2981–2999.
- Ansari, A., 1999. Prediction of multicomponent inorganic atmospheric aerosol behavior. *Atmos. Environ.* 33 (5), 745–757. [http://dx.doi.org/10.1016/S1352-2310\(98\)00221-0](http://dx.doi.org/10.1016/S1352-2310(98)00221-0), URL <https://linkinghub.elsevier.com/retrieve/pii/S1352231098002210>.
- Aouizerats, B., Thouron, O., Tulet, P., Mallet, M., Gomes, L., Henzing, J.S., 2010. Development of an online radiative module for the computation of aerosol optical properties in 3-D atmospheric models: validation during the EUCAARI campaign. *Geosci. Model Dev.* 3 (2), 553–564. <http://dx.doi.org/10.5194/gmd-3-553-2010>.
- Baklanov, A., Brunner, D., Carmichael, G., Flemming, J., Freitas, S., Gauss, M., Hov, Ø., Mathur, R., Schlünzen, K.H., Seigneur, C., Vogel, B., 2017. Key issues for seamless integrated chemistry–meteorology modeling. *Bull. Am. Meteorol. Soc.* 98 (11), 2285–2292. <http://dx.doi.org/10.1175/bams-d-15-00166.1>.
- Baklanov, A., Schlünzen, K., Suppan, P., Baldasano, J., Brunner, D., Aksoyoglu, S., Carmichael, G., Douros, J., Flemming, J., Forkel, R., Galmarini, S., Gauss, M., Grell, G., Hirtl, M., Joffre, S., Jorba, O., Kaas, E., Kaasik, M., Kallos, G., Kong, X., Korsholm, U., Kurganskiy, A., Kushta, J., Lohmann, U., Mahura, A., Manders-Groot, A., Maurizi, A., Moussiopoulos, N., Rao, S.T., Savage, N., Seigneur, C., Sokhi, R.S., Solazzo, E., Solomos, S., Sørensen, B., Tsegas, G., Vignati, E., Vogel, B., Zhang, Y., 2014. Online coupled regional meteorology chemistry models in Europe: current status and prospects. *Atmos. Chem. Phys.* 14 (1), 317–398. <http://dx.doi.org/10.5194/acp-14-317-2014>, URL <https://acp.copernicus.org/articles/14/317/2014/>.
- Bessagnet, B., Beauchamp, M., Guerreiro, C., De Leeuw, F., Tsyro, S., Colette, A., Meleux, F., Rouil, L., Ruysenaars, P., Sauter, F., Velders, G.J., Foltescu, V.L., Van Aardenne, J., 2014. Can further mitigation of ammonia emissions reduce exceedances of particulate matter air quality standards? *Environ. Sci. Policy* 44, 149–163. <http://dx.doi.org/10.1016/j.envsci.2014.07.011>, URL <https://linkinghub.elsevier.com/retrieve/pii/S1462901114001348>.
- Bessagnet, B., Cuvelier, K., De Meij, A., Monteiro, A., Pisoni, E., Thunis, P., Violaris, A., Kushta, J., Denby, B.R., Mu, Q., Wærsted, E.G., Vivanco, M.G., Theobald, M.R., Gil, V., Sokhi, R.S., Momoh, K., Alyuz, U., Vpm, R., Kumar, S., Bossioli, E., Methy-maki, G., Brzaja, D., Milić, V., Cholokian, A., Pennel, R., Mailler, S., Menut, L., Briganti, G., Mircea, M., Flandorfer, C., Baumann-Stanzer, K., Hutsemékers, V., Trimpeers, E., 2023. Assessment of the sensitivity of model responses to urban emission changes in support of emission reduction strategies. *Air Qual., Atmos. Health* <http://dx.doi.org/10.1007/s11869-023-01469-z>, URL <https://link.springer.com/10.1007/s11869-023-01469-z>.
- Bessagnet, B., Menut, L., Lapere, R., Couvidat, F., Jaffrezo, J.-L., Mailler, S., Favez, O., Pennel, R., Siour, G., 2020. High resolution chemistry transport modeling with the on-line CHIMERE-WRF model over the French Alps—Analysis of a feedback of surface particulate matter concentrations on mountain meteorology. *Atmosphere* 11 (6), 565. <http://dx.doi.org/10.3390/atmos11060565>, URL <https://www.mdpi.com/2073-4433/11/6/565>.
- Bossioli, E., Tombrou, M., Dandou, A., Soukallakis, N., 2007. Simulation of the effects of critical factors on ozone formation and accumulation in the greater Athens area. *J. Geophys. Res.: Atmos.* 112 (D2), <http://dx.doi.org/10.1029/2006jd007185>.
- Brands, S., Fernández-García, G., García Vivanco, M., Tesouro Montecelo, M., Gallego Fernández, N., Saunders Estévez, A.D., Carracedo García, P.E., Neto Venâncio, A., Melo Da Costa, P., Costa Tomé, P., Otero, C., Macho, M.L., Taboada, J., 2020. An exploratory performance assessment of the CHIMERE model (version 2017r4) for the northwestern Iberian peninsula and the summer season. *Geosci. Model Dev.* 13 (9), 3947–3973.
- Carter, W.P., 2010. Development of the SAPRC-07 chemical mechanism. *Atmos. Environ.* 44 (40), 5324–5335. <http://dx.doi.org/10.1016/j.atmosenv.2010.01.026>, URL <https://linkinghub.elsevier.com/retrieve/pii/S1352231010000646>.
- Carter, W.P.L., Winer, A.M., Pitts, Jr., J.N., 1982. Effects of kinetic mechanisms and hydrocarbon composition on oxidant-precursor relationships predicted by the ekma isopleth technique. *Atmos. Environ.* 16 (1), 113–120.
- CESM, 2019. CESM2.1/CAM-chem instantaneous output for boundary conditions. <http://dx.doi.org/10.5065/NMP7-EP60>, URL <https://wiki.ucar.edu/display/camchem/CESM2.1%3ACAM-chem+as+Boundary+Conditions>.
- Chan, Y.-C., Evans, M.J., He, P., Holmes, C.D., Jaeglé, L., Kasibhatla, P., Liu, X.-Y., Sherwen, T., Thornton, J.A., Wang, X., Xie, Z., Zhai, S., Alexander, B., 2021. Heterogeneous nitrate production mechanisms in intense haze events in the north China plain. *J. Geophys. Res.: Atmos.* 126 (9), <http://dx.doi.org/10.1029/2021jd034688>.
- Chen, C.-H., Chen, T.-F., Huang, S.-P., Chang, K.-H., 2021. Comparison of the RADM2 and RACM chemical mechanisms in O3 simulations: effect of the photolysis rate constant. *Sci. Rep.* 11 (1), 5024. <http://dx.doi.org/10.1038/s41598-021-84629-4>, URL <https://www.nature.com/articles/s41598-021-84629-4>.
- Cholakian, A., Bessagnet, B., Menut, L., Pennel, R., Mailler, S., 2023. Anthropogenic emission scenarios over Europe with the WRF-CHIMERE-v2020 models: Impact of duration and intensity of reductions on surface concentrations during the winter of 2015. *Atmosphere (Basel)* 14 (2), 224.
- Colette, A., Bessagnet, B., Meleux, F., Terrenoire, E., Rouil, L., 2014. Frontiers in air quality modelling. *Geosci. Model Dev.* 7 (1), 203–210. <http://dx.doi.org/10.5194/gmd-7-203-2014>, URL <https://gmd.copernicus.org/articles/7/203/2014/>.
- Curci, G., 2012. On the impact of time-resolved boundary conditions on the simulation of surface ozone and PM10. In: *Air Pollution - Monitoring, Modelling, Health and Control*. InTech.
- Damian, V., Sandu, A., Damian, M., Potra, F., Carmichael, G.R., 2002. The kinetic preprocessor KPP—a software environment for solving chemical kinetics. *Comput. Chem. Eng.* 26 (11), 1567–1579. [http://dx.doi.org/10.1016/S0098-1354\(02\)00128-x](http://dx.doi.org/10.1016/S0098-1354(02)00128-x).
- De Meij, A., Cuvelier, C., Thunis, P., Pisoni, E., Bessagnet, B., 2024. Sensitivity of air quality model responses to emission changes: comparison of results based on four EU inventories through FAIRMODE benchmarking methodology. *Geosci. Model Dev.* 17 (2), 587–606. <http://dx.doi.org/10.5194/gmd-17-587-2024>, URL <https://gmd.copernicus.org/articles/17/587/2024/>.
- Eder, B., Kang, D., Rao, S.T., Mathur, R., Yu, S., Otte, T., Schere, K., Wayland, R., Jackson, S., Davidson, P., McQueen, J., Bridgers, G., 2010. Using national air quality forecast guidance to develop local air quality index forecasts. *Bull. Am. Meteorol. Soc.* 91 (3), 313–326. <http://dx.doi.org/10.1175/2009BAMS2734.1>, URL <https://journals.ametsoc.org/doi/10.1175/2009BAMS2734.1>.
- Eder, B., Yu, S., 2006. A performance evaluation of the 2004 release of models-3 CMAQ. *Atmos. Environ.* 40 (26), 4811–4824. <http://dx.doi.org/10.1016/j.atmosenv.2005.08.045>, URL <https://linkinghub.elsevier.com/retrieve/pii/S1352231006000926>.
- EEA, 2023. Air Pollution in Europe: 2023 Reporting Status Under the National Emission Reduction Commitments Directive. Publications Office, LU, URL <https://data.europa.eu/doi/10.2800/339055>, last access 28/01/2024.
- Forkel, R., Balzarini, A., Baró, R., Bianconi, R., Curci, G., Jiménez-Guerrero, P., Hirtl, M., Honzak, L., Lorenz, C., Im, U., Pérez, J.L., Pirovano, G., San José, R., Tuccella, P., Werhahn, J., Žabkar, R., 2015. Analysis of the WRF-Chem contributions to AQMEII phase2 with respect to aerosol radiative feedbacks on meteorology and pollutant distributions. *Atmos. Environ.* 115, 630–645. <http://dx.doi.org/10.1016/j.atmosenv.2014.10.056>.
- Granier, C., Darras, S., Denier van der Gon, H., Doubalova, J., Elguindi, N., Galle, B., Gauss, M., Guevara, M., Jalkanen, J.-P., Kuenen, J., Liousse, C., Quack, B., Simpson, D., Sindelarova, K., 2019. The copernicus atmosphere monitoring service global and regional emissions (April 2019 version).
- Grell, G.A., Dévényi, D., 2002. A generalized approach to parameterizing convection combining ensemble and data assimilation techniques. *Geophys. Res. Lett.* 29 (14), 38–1–38–4.
- Grell, G.A., Peckham, S.E., Schmitz, R., McKeen, S.A., Frost, G., Skamarock, W.C., Eder, B., 2005. Fully coupled “online” chemistry within the WRF model. *Atmos. Environ.* (1994) 39 (37), 6957–6975.
- Gross, A., Stockwell, W.R., 2003. [No title found]. *J. Atmos. Chem.* 44 (2), 151–170. <http://dx.doi.org/10.1023/A:1022483412112>, URL <http://link.springer.com/10.1023/A:1022483412112>.
- Guenther, A., Karl, T., Harley, P., Wiedinmyer, C., Palmer, P.I., Geron, C., 2006. Estimates of global terrestrial isoprene emissions using MEGAN (Model of Emissions of Gases and Aerosols from Nature). *Atmos. Chem. Phys.* 6 (11), 3181–3210.
- He, J., Glotfelty, T., Yahya, K., Alapaty, K., Yu, S., 2017. Does temperature nudging overwhelm aerosol radiative effects in regional integrated climate models? *Atmos. Environ.* 154, 42–52. <http://dx.doi.org/10.1016/j.atmosenv.2017.01.040>, URL <https://www.sciencedirect.com/science/article/pii/S1352231017300481>.
- Hong, S.-Y., Noh, Y., Dudhia, J., 2006. A new vertical diffusion package with an explicit treatment of entrainment processes. *Mon. Weather Rev.* 134 (9), 2318–2341.
- Iacono, M.J., Delamere, J.S., Mlawer, E.J., Shephard, M.W., Clough, S.A., Collins, W.D., 2008. Radiative forcing by long-lived greenhouse gases: Calculations with the AER radiative transfer models. *J. Geophys. Res.* 113 (D13).
- Im, U., Christensen, J.H., Geels, C., Hansen, K.M., Brandt, J., Solazzo, E., Alyuz, U., Balzarini, A., Baro, R., Bellasio, R., Bianconi, R., Bieser, J., Colette, A., Curci, G., Farrow, A., Flemming, J., Fraser, A., Jimenez-Guerrero, P., Kitwiroon, N., Liu, P., Nopmongkol, U., Palacios-Peña, L., Pirovano, G., Pozzoli, L., Prank, M., Rose, R., Sokhi, R., Tuccella, P., Unal, A., Vivanco, M.G., Yarwood, G., Hogrefe, C., Galmarini, S., 2018. Influence of anthropogenic emissions and boundary conditions on multi-model simulations of major air pollutants over Europe and North America in the framework of AQMEII3. *Atmos. Chem. Phys.* 18 (12), 8929–8952.

- Janssens-Maenhout, G., Crippa, M., Guizzardi, D., Dentener, F., Muntean, M., Pouliot, G., Keating, T., Zhang, Q., Kurokawa, J., Wankmüller, R., Denier van der Gon, H., Kuenen, J.J.P., Klimont, Z., Frost, G., Darras, S., Koffi, B., Li, M., 2015. HTAP_v2.2: a mosaic of regional and global emission grid maps for 2008 and 2010 to study hemispheric transport of air pollution. *Atmos. Chem. Phys.* 15 (19), 11411–11432.
- Kruse, C.G., Bacmeister, J.T., Zarzycki, C.M., Larson, V.E., Thayer-Calder, K., 2022. Do nudging tendencies depend on the nudging timescale chosen in atmospheric models? *J. Adv. Modelling Earth Syst.* 14 (10), <http://dx.doi.org/10.1029/2022MS003024>, e2022MS003024 2022MS003024, arXiv:<https://agupubs.onlinelibrary.wiley.com/doi/pdf/10.1029/2022MS003024>, URL <https://agupubs.onlinelibrary.wiley.com/doi/abs/10.1029/2022MS003024>.
- Kushta, J., Georgiou, G.K., Proestos, Y., Christoudias, T., Thunis, P., Savvides, C., Papadopoulos, C., Lelieveld, J., 2019. Evaluation of EU air quality standards through modeling and the FAIRMODE benchmarking methodology. *Air Qual. Atmos. Health* 12 (1), 73–86.
- Lapere, R., Menut, L., Mailler, S., Huneuev, N., 2021. Seasonal variation in atmospheric pollutants transport in central Chile: dynamics and consequences. *Atmos. Chem. Phys.* 21 (8), 6431–6454.
- Li, K., Jacob, D.J., Liao, H., Zhu, J., Shah, V., Shen, L., Bates, K.H., Zhang, Q., Zhai, S., 2019. A two-pollutant strategy for improving ozone and particulate air quality in China. *Nat. Geosci.* 12 (11), 906–910. <http://dx.doi.org/10.1038/s41561-019-0464-x>.
- Mailler, S., Menut, L., Khvorostyanov, D., Valari, M., Couvidat, F., Siour, G., Turquety, S., Briant, R., Tuccella, P., Bessagnet, B., Colette, A., Létinois, L., Markakis, K., Meleux, F., 2017. CHIMERE-2017: from urban to hemispheric chemistry-transport modeling. *Geosci. Model Dev.* 10 (6), 2397–2423. <http://dx.doi.org/10.5194/gmd-10-2397-2017>, URL <https://gmd.copernicus.org/articles/10/2397/2017/>.
- Mareckova, K., Pinteris, M., Ullrich, B., Wankmueller, R., Gaisbauer, S., 2019. Review of emission data reported under the LRTAP Convention and the NEC Directive Stage 1 and 2 review Status of gridded and LPS data. EMEP report 4/2019, Umweltbundesamt GmbH, Vienna, Austria, URL https://www.ceip.at/fileadmin/inhalte/ceip/00_pdf_other/2019/inventoryreport_2019.pdf.
- Menut, L., Bessagnet, B., Briant, R., Cholakian, A., Couvidat, F., Mailler, S., Pennel, R., Siour, G., Tuccella, P., Turquety, S., Valari, M., 2021. The CHIMERE v2020r1 online chemistry-transport model. *Geosci. Model Dev.* 14 (11), 6781–6811. <http://dx.doi.org/10.5194/gmd-14-6781-2021>, URL <https://gmd.copernicus.org/articles/14/6781/2021/>.
- Menut, L., Bessagnet, B., Siour, G., Mailler, S., Pennel, R., Cholakian, A., 2020. Impact of lockdown measures to combat Covid-19 on air quality over western Europe. *Sci. Total Environ.* 741, 140426. <http://dx.doi.org/10.1016/j.scitotenv.2020.140426>, URL <https://linkinghub.elsevier.com/retrieve/pii/S0048969720339486>.
- Menut, L., Tuccella, P., Flamant, C., Deroubaix, A., Gaetani, M., 2019. The role of aerosol–radiation–cloud interactions in linking anthropogenic pollution over southern west Africa and dust emission over the Sahara. *Atmos. Chem. Phys.* 19 (23), 14657–14676. <http://dx.doi.org/10.5194/acp-19-14657-2019>.
- Methymaki, G., Bossioli, E., Boucouvala, D., Nenes, A., Tombrou, M., 2023. Brown carbon absorption in the Mediterranean basin from local and long-range transported biomass burning air masses. *Atmos. Environ.* 306, 119822. <http://dx.doi.org/10.1016/j.atmosenv.2023.119822>.
- Morrison, H., Curry, J.A., Shupe, M.D., Zuidema, P., 2005. A new double-moment microphysics parameterization for application in cloud and climate models. Part II: Single-column modeling of arctic clouds. *J. Atmos. Sci.* 62 (6), 1678–1693. <http://dx.doi.org/10.1175/JAS3447.1>, URL <https://journals.ametsoc.org/view/journals/atsc/62/6/jas3447.1.xml>.
- NOAA, 2015. NCEP GDAS/FNL 0.25 degree global tropospheric analyses and forecast grids. <http://dx.doi.org/10.5065/D65Q4T4Z>, URL <http://rda.ucar.edu/datasets/ds083.3/>.
- Otte, T.L., Nolte, C.G., Otte, M.J., Bowden, J.H., 2012. Does nudging squelch the extremes in regional climate modeling? *J. Clim.* 25 (20), 7046–7066. <http://dx.doi.org/10.1175/JCLI-D-12-00048.1>, URL <https://journals.ametsoc.org/view/journals/clim/25/20/jcli-d-12-00048.1.xml>.
- Russell, A., 2000. NARSTO critical review of photochemical models and modeling. *Atmos. Environ.* 34 (12–14), 2283–2324. [http://dx.doi.org/10.1016/s1352-2310\(99\)00468-9](http://dx.doi.org/10.1016/s1352-2310(99)00468-9).
- Sandu, A., Sander, R., 2006. Technical note: Simulating chemical systems in Fortran90 and Matlab with the Kinetic PreProcessor KPP-2.1. *Atmos. Chem. Phys.* 6 (1), 187–195. <http://dx.doi.org/10.5194/acp-6-187-2006>.
- Skamarock, W., Klemp, J., Dudhia, J., Gill, D., Barker, D., Wang, W., Huang, X.-Y., Duda, M., 2008. A Description of the Advanced Research WRF Version 3.
- Stockwell, W.R., Kirchner, F., Kuhn, M., Seefeld, S., 1997. A new mechanism for regional atmospheric chemistry modeling. *J. Geophys. Res.: Atmos.* 102 (D22), 25847–25879. <http://dx.doi.org/10.1029/97JD00849>, URL <https://agupubs.onlinelibrary.wiley.com/doi/10.1029/97JD00849>.
- Stockwell, W.R., Middleton, P., Chang, J.S., Tang, X., 1990. The second generation regional acid deposition model chemical mechanism for regional air quality modeling. *J. Geophys. Res.: Atmos.* 95 (D10), 16343–16367. <http://dx.doi.org/10.1029/JD095iD10p16343>, URL <https://agupubs.onlinelibrary.wiley.com/doi/10.1029/JD095iD10p16343>.
- Thunis, P., Clappier, A., 2014. Indicators to support the dynamic evaluation of air quality models. *Atmos. Environ.* 98, 402–409. <http://dx.doi.org/10.1016/j.atmosenv.2014.09.016>, URL <https://linkinghub.elsevier.com/retrieve/pii/S1352231014007092>.
- Thunis, P., Pisoni, E., Degraeuwe, B., Kranenburg, R., Schaap, M., Clappier, A., 2015. Dynamic evaluation of air quality models over European regions. *Atmos. Environ.* 111, 185–194. <http://dx.doi.org/10.1016/j.atmosenv.2015.04.016>, URL <https://linkinghub.elsevier.com/retrieve/pii/S1352231015300194>.
- Vivanco, M.G., Palomino, I., Vautard, R., Bessagnet, B., Martín, F., Menut, L., Jiménez, S., 2009. Multi-year assessment of photochemical air quality simulation over Spain. *Environ. Model. Softw.* 24 (1), 63–73. <http://dx.doi.org/10.1016/j.envsoft.2008.05.004>, URL <https://linkinghub.elsevier.com/retrieve/pii/S136481520800090X>.
- WHO, 2021. WHO global air quality guidelines: particulate matter (PM_{2.5} and PM₁₀), ozone, nitrogen dioxide, sulfur dioxide and carbon monoxide. Technical Report, WHO, Geneva, p. 267, URL <https://apps.who.int/iris/handle/10665/345329>, Licence: CC BY-NC-SA 3.0 IGO, last access: 28/01/2024.
- WHO, 2023. Overview of Methods to Assess Population Exposure to Ambient Air Pollution. Geneva, URL <https://www.who.int/publications/i/item/9789240073494>, last access: 28/01/2024.